

On the symmetry and crystal structure of aguilarite, Ag_4SeS

L. BINDI^{1,2,*} AND N. E. PINGITORE³

¹ Dipartimento di Scienze della Terra, Università degli Studi di Firenze, Via G. La Pira 4, I-50121 Firenze, Italy

² CNR – Istituto di Geoscienze e Georisorse, Sezione di Firenze, Via G. La Pira 4, I-50121 Firenze, Italy

³ Department of Geological Sciences, The University of Texas at El Paso, El Paso, TX-79968-0555 Texas, USA

[Received 10 December 2012; Accepted 9 January 2013; Associate Editor: Giancarlo Della Ventura]

ABSTRACT

An examination of a specimen of aguilarite from the type locality provides new data on the chemistry and structure of this mineral. The chemical formula of the crystal used for the structural study is $(\text{Ag}_{3.98}\text{Cu}_{0.02})(\text{Se}_{0.98}\text{S}_{0.84}\text{Te}_{0.18})$, on the basis of 6 atoms. The mineral was found to be monoclinic, crystallizing in space group $P2_1/n$, with $a = 4.2478(2)$, $b = 6.9432(3)$, $c = 8.0042(5)$ Å, $\beta = 100.103(2)^\circ$, $V = 232.41(2)$ Å³ and $Z = 4$. The crystal structure [refined to $R_1 = 0.0139$ for 958 reflections with $I > 2\sigma(I)$] is topologically identical to that of acanthite, Ag_2S . It can be described as a body-centred array of tetrahedrally coordinated X atoms ($X = \text{S}, \text{Se}$ and Te) with Ag_2X_3 triangles in planes nearly parallel to (010); the sheets are linked by the Ag1 silver site, which has twofold coordination.

Aguilarite is definitively proved to be isostructural with acanthite; it does not have a naumannite-like structure, as previously supposed. Our data support the hypothesis that there are two solid solution series in the system: a monoclinic ‘acanthite-like’ series (from $\text{Ag}_2\text{S}-\text{Ag}_2\text{S}_{0.4}\text{Se}_{0.6}$), and an orthorhombic ‘naumannite-like’ series (from $\text{Ag}_2\text{S}_{0.3}\text{Se}_{0.7}-\text{Ag}_2\text{Se}$). This is supported by data gathered on synthetic counterparts. Aguilarite remains as a valid as a mineral species, but it should be described as the Se-analogue of acanthite.

In this study we also (1) review the history of the aguilarite; (2) compare properties of synthetic and natural aguilarite; and (3) demonstrate how earlier researchers erred in describing aguilarite as orthorhombic.

The Te-bearing composition of the studied aguilarite crystal suggests the possibility of a solid solution with cervelleite (Ag_4TeS).

KEYWORDS: aguilarite, crystal structure, Ag-sulfides, acanthite, naumannite, cervelleite, Mexico.

Introduction

THE system $\text{Ag}_2\text{S}-\text{Ag}_2\text{Se}$ has recently attracted significant attention in materials research due to its optical, electrical and thermoelectric properties (e.g. Xiao *et al.*, 2012); it has been of considerable interest in mineral sciences for many years due to the importance of the minerals involved. At ambient conditions these are: acanthite, Ag_2S , which is monoclinic, space group $P2_1/n$ according to Frueh (1958); naumannite, Ag_2Se , which is orthorhombic, space group $P2_12_12_1$ according to

Wiegiers (1971); and the intermediate member aguilarite (Genth, 1891, 1892), Ag_4SeS , which is orthorhombic according to Petruk *et al.* (1974) and is listed as such in several mineralogical databases (e.g. www.webmineral.com; www.mindat.org), although there are no detailed structural studies. According to Pingitore *et al.* (1992, 1993), these three semiconductor phases undergo structural transitions to a cubic high-temperature conductive form in the temperature range 70–178°C, depending on their composition.

The possible solid solution between Ag_2S and Ag_2Se has been debated for a long time. Indeed, chemical analyses reported in the scientific literature for acanthite and naumannite support

* E-mail: luca.bindi@unifi.it

DOI: 10.1180/minmag.2013.077.1.03

the solid-solution argument. Moreover, cervelleite, Ag_4TeS (Criddle *et al.*, 1989) was reported to contain selenium (Spry and Thieben, 1996) thus suggesting the possibility of solid solution with aguilarite (Ag_4SeS).

To examine the extent of solid solution in the system $\text{Ag}_2\text{S}-\text{Ag}_2\text{Se}$ at ambient conditions, Pingitore *et al.* (1992) carried out a careful experimental study of 80 experimental charges with compositions ranging from Ag_2S to Ag_2Se by optical microscopy, electron-probe microanalysis and X-ray diffraction. The main conclusions were that the intermediate member, aguilarite, could be considered to be Se-rich acanthite, with the same monoclinic crystal structure, and that at ambient conditions there are two solid solutions [i.e. the $\text{Ag}_2\text{S}-\text{Ag}_2\text{S}_{0.4}\text{Se}_{0.6}$ monoclinic series and $\text{Ag}_2\text{S}_{0.3}\text{Se}_{0.7}-\text{Ag}_2\text{Se}$ orthorhombic series]. Pingitore *et al.* (1992) also pointed out that the status of aguilarite as a mineral species could be called into question as it was erroneously thought to be orthorhombic by Petruk *et al.* (1974). The conclusions drawn by Pingitore *et al.* (1992), however, have not been demonstrated for natural samples.

To resolve concerns relating to the *status* of aguilarite, structural, physical and chemical data for the mineral from the type locality, San Carlos mine, Guanajuato, Mexico, are reported herein.

Aguilarite review

Early studies of aguilarite

Aguilarite was described by Genth (1891, 1892) and named after Mr P. Aguilar, who was the superintendent of San Carlos Mine, Guanajuato, Mexico, which is the type locality. The initial description predates both X-ray diffraction and electron-probe microanalysis.

X-ray powder diffraction data, consisting of ten *d*-spacings with their relative intensities, were first reported for aguilarite from Guanajuato, Mexico by Harcourt (1942). A systematic investigation of selenide minerals, which includes X-ray powder diffraction photographs of both aguilarite and synthetic Ag_4SeS , along with a table of intensities, peak angles and lattice spacings for the latter was subsequently reported by Earley (1950). Earley commented on the similarities between the peaks of aguilarite, those of synthetic Ag_4SeS and those reported by Harcourt (1942). He concluded that because the X-ray powder patterns of aguilarite and synthetic Ag_4SeS showed only "faint resemblances" to those of

naumannite and acanthite, aguilarite was a distinct mineral species. In particular, he specifically rejected the suggestion of Schneiderhöhn and Ramdohr (1931), that aguilarite was a member of the acanthite–naumannite series.

In a review of selenium in epithermal deposits, Davidson (1960) repeated the suggestion that there was a solid solution from acanthite to naumannite. This was based on the similarity in the radii of Se^{2-} and S^{2-} anions, and on the substitution of these anions in solid solutions of related minerals. Main *et al.* (1972) examined aguilarite from a hydrothermal vein deposit in New Zealand, a sample from Guanajuato (Mexico), and synthetic Ag_4SeS . On the basis of X-ray powder diffraction studies of the last two of these, they suggested that some of the diffraction peaks reported by Earley (1950) were in error. They also reported the elemental composition of a single grain of the New Zealand material by electron-probe microanalysis. Differential thermal analysis of a galena-aguilarite concentrate and of their synthetic material each yielded an endotherm with a maximum at 122°C. This endotherm represents the transition to a high-temperature solid phase, which corresponds to those reported for acanthite (176°C) and naumannite (133°C). Main *et al.* (1971) concluded that the available X-ray data were insufficient to permit confident indexing of the aguilarite powder pattern.

The cornerstone investigation of Petruk *et al.* (1974)

For the past four decades, the data, literature review and phase diagram presented by Petruk *et al.* (1974) have served as the foundation for studies of the mineralogy and behaviour of the silver–sulfur–selenium system. These authors examined aguilarite and acanthite from Guanajuato, Mexico, and naumannite from Silver City, Idaho, USA, by ore microscopy (with etching), electron-probe microanalysis and X-ray powder diffraction. The X-ray diffraction pattern of aguilarite was indexed on a naumannite-type orthorhombic cell. On the basis of these data, previously published elemental analyses, and their interpretation of the parageneses of their mineral suites, Petruk *et al.* (1974) made the assertion that acanthite, aguilarite and naumannite are distinct mineral species. They suggested molar compositional limits for sulfur–selenium substitutions of up to 0.15 Se in acanthite, 0.025 Se or

0.05 S in aguilarite (converted here to an Ag_2X -type formula for comparative purposes), and 0.12 S in naumannite. They also suggested that these compositional ranges are separated by two fields where a presumed high-temperature cubic solid solution destabilizes between 176 and 115°C to form intergrowths of the two appropriate minerals (acanthite–aguilarite or aguilarite–naumannite).

Further studies

Shikazono (1978) documented various compositions between acanthite and aguilarite outside the substitutional limits suggested by Petruk *et al.* (1974). Shikazono concluded that if those limits were correct, his materials must be intergrowths of acanthite and aguilarite. Morales and Borodayev (1982) reported microprobe analyses of a range of compositions between acanthite and aguilarite from a segment of the Veta Madre (Las Torres area) in Guanajuato. Backscattered-electron images and X-ray mapping showed that the small (10–100 μm) grains they examined were monomineralic, rather than intergrowths of acanthite and aguilarite. They concluded that a continuous isomorphous solid solution must exist between acanthite and aguilarite, suggesting that Petruk *et al.* (1974) had been misled by their reliance on etching and broad-beam (15–80 μm) probe analyses. These investigators did not, however, address the structural problem: acanthite is monoclinic, whereas aguilarite was supposed to be orthorhombic. The isomorphous solid solution that they proposed is, therefore, logically impossible.

Samples studied

The San Carlos sample containing aguilarite used for the structural study reported herein is from the Gem and Mineral Collection of the Department of Geosciences at Princeton University, which consists of approximately 6000 catalogued mineral specimens and several hundred cut gemstones that were collected from the 1820s to the 1970s, together with historic documents and rare specimen labels from early mineral dealers, recording the growth and development of mineral collecting and its interaction with the scientific community.

The label associated with the sample used for the structural study reads: “*aguilarite, Ag₄SeS, San Carlos mine, Mexico*” (catalogue number I/53a/2312). Unfortunately, we are unable to

provide additional information about the sample, but, based on the writing style on the index card, it was probably catalogued in the 1920s. On the small vial containing the sample there is a tiny price tag “\$1.00” in the style of Ward’s old labels. This makes sense as, shortly after the formal establishment of the Department of Geology (as it was known then) in 1904, Professor Alexander Phillips, who occupied the chair in mineralogy in the period 1905–1936, led an effort to greatly expand the collection through purchases, assembling a comprehensive teaching and reference collection consisting of nearly all the minerals known at the time with an emphasis on specimens from type localities.

The sample mainly consists of aguilarite associated with a very small amount of acanthite. The aguilarite exhibits a subhedral to anhedral grain morphology, and does not show any inclusions of, or intergrowths with, other minerals. The maximum aguilarite grain size is ~250 μm .

Aguilarite samples 48a.2 and 48a.6 from the ‘Pennsylvania Genth San Carlos collection’ of Pennsylvania State University were examined independently in the laboratory of the Department of Geological Sciences of the University of Texas. It is possible that these are cotype specimens and they may be from the original (presumed lost) type specimen, given the provenance, and in the absence of other claims as to the whereabouts of the type specimen. Specimens from the National Museum of Natural History (Washington D.C.), with registration numbers USNMNH C 380 (Canfield Collection, pre-1927, from the San Carlos mine) and 93436 were also examined.

Physical and optical properties

Aguilarite is black with a dark brown-black streak. The mineral is opaque in transmitted light and has a metallic lustre. No cleavage is present and the fracture is uneven. Micro-indentation hardness measurements carried out on the specimen used in the structural study with a load (VHN) of 25 g give a mean value of 21 kg mm^{-2} (range: 19–23) corresponding to a Mohs hardness of 1–1½.

In plane-polarized incident light, aguilarite is dark grey in colour, moderately bireflectant and not pleochroic. Between crossed polars, aguilarite is very weakly anisotropic with greyish to light-green rotation tints. Internal reflections are absent

and there is no optical evidence of growth zonation.

Reflectance measurements were performed in air by means of a MPM-200 Zeiss microphotometer equipped with a MSP-20 system processor on a Zeiss Axioplan ore microscope. The filament temperature was approximately 3350 K. An interference filter was adjusted, in turn, to select four wavelengths for measurement (471.1, 548.3, 586.6, and 652.3 nm). Measurements were made on an area of the specimen 0.1 mm in diameter and on a silicon carbide standard under the same focussing conditions. Reflectance percentages, R_{\min} and R_{\max} , are: 34.2, 34.7 (471.1 nm); 33.9, 34.5 (548.3 nm); 32.7, 33.9 (586.6 nm); and 30.8,

31.3 (652.3 nm), respectively, in excellent agreement with the values reported by Stanley and Gooday in Criddle and Stanley (1993).

X-ray crystallography and crystal-structure refinement

A small crystal fragment ($80 \times 65 \times 55 \mu\text{m}$) was selected from specimen I/53a/2312 for a single-crystal X-ray diffraction study using an Oxford Diffraction Xcalibur 3 CCD single-crystal diffractometer (Table 1). Surprisingly, the unit-cell parameters determined for the selected crystal indicated monoclinic symmetry, with $a \sim 4.25$, $b \sim 6.94$, $c \sim 8.00 \text{ \AA}$ and $\beta \sim 110^\circ$, which are very

TABLE 1. Crystallographic data and refinement parameters for agularite (sample # I/53a/2312).

Crystal data	
Ideal formula	Ag ₄ SeS
Crystal system	monoclinic
Space group	$P2_1/n$
Unit-cell parameters (\AA , $^\circ$)	4.2478(2) 6.9432(3) 8.0042(5)
Unit-cell volume (\AA^3)	90.00 100.103(2) 90.00
Z	232.41(2)
Crystal size (mm)	4
	0.080 \times 0.065 \times 0.055
Data collection	
Diffractometer	Oxford Xcalibur 3
Temperature (K)	298(3)
Radiation, wavelength (\AA)	MoK α , 0.71073
2 θ max for data collection ($^\circ$)	69.94
Crystal-detector dist. (mm)	50
h, k, l ranges	$-6 \leq h \leq 6, -11 \leq k \leq 11, -12 \leq l \leq 12$
Axis, frames, width ($^\circ$), time per frame (s)	ω - ϕ , 1152, 1.00, 25
Total reflections collected	3832
Unique reflections (R_{int})	958 (0.066)
Unique reflections $I > 2\sigma(I)$	520
Data completeness to θ_{max} (%)	99.6
Absorption correction method	ABSPACK (Oxford Diffraction, 2006)
Structure refinement	
Refinement method	Full-matrix least-squares on F^2
Data/restraints/parameters	958/0/29
R_1 [$I > 2\sigma(I)$], wR_2 [$I > 2\sigma(I)$]	0.0139, 0.0305
R_1 all, wR_2 all	0.0152, 0.0306
Goodness-of-fit on F^2	0.223
Largest diff. peak and hole ($\text{e}^- \text{\AA}^{-3}$)	1.26, -1.41

$$R_{\text{int}} = (n/n - 1)^{1/2} [F_o^2 - F_o(\text{mean})^2] / \Sigma F_o^2$$

$$R_1 = \Sigma |F_o| - |F_c| / \Sigma |F_o|; wR_2 = \{ \Sigma [w(F_o^2 - F_c^2)^2] / \Sigma [w(F_o^2)^2] \}^{1/2};$$

$$w = 1 / [\sigma^2(F_o^2) + (aP)^2 + bP], \text{ where } P = (\max(F_o^2, 0) + 2F_c^2) / 3;$$

$$\text{Goof} = \{ \Sigma [w(F_o^2 - F_c^2)^2] / (n - p) \}^{1/2}$$

where n is the number of reflections and p is the number of refined parameters.

CRYSTAL STRUCTURE OF AGUILARITE

 TABLE 2. Atoms, Wyckoff letter, site occupancy, fractional atom coordinates, and isotropic atomic displacement parameters (\AA^2) for aguilarite (sample # I/53a/2312).

Atom	Wyckoff	Site occupancy	x/a	y/b	z/c	U_{eq}
Ag1	4e	Ag _{1.00}	0.75442(6)	0.01378(4)	0.30116(2)	0.01762(6)
Ag2	4e	Ag _{1.00}	0.28840(6)	0.31874(4)	0.43144(2)	0.01803(6)
X	4e	S _{0.333(3)} Se _{0.667}	0.3603(1)	0.24110(7)	0.13054(4)	0.0216(1)

close to those of acanthite (Frueh, 1958). Systematic absences ($h0l$: $h + l = 2n$; $h00$: $h = 2n$; $0k0$: $k = 2n$; $00l$: $l = 2n$) are consistent with space group $P2_1/n$ ($P2_1/c$ as standard). Statistical tests on the distribution of $|E|$ values strongly indicate the presence of an inversion centre ($|E^2 - 1| = 0.893$), supporting the choice of space group $P2_1/n$. It was therefore decided to refine the aguilarite structure in the non-standard space group $P2_1/n$ in order to have the same orientation reported for acanthite. The program *SHELXL* (Sheldrick, 2008) was used to refine the structure, starting from the atom coordinates listed by Frueh (1958) for acanthite. The occupancy of all the sites was left free to vary (Ag vs. vacancy; S vs. Se) and then fixed to the resulting value. The refined values are listed in Table 2. Neutral scattering curves for Ag, S and Se were taken from the *International Tables for X-ray Crystallography* (Ibers and Hamilton, 1974). At the last stage of refinement, with anisotropic atomic-displacement parameters for all atoms and no constraints, the residual value settled at $R = 0.0139$ for 520 observed reflections [$2\sigma(I)$ level] and 29 parameters and at $R = 0.0152$ for all 958 independent reflections. Experimental details and R indices are listed in Table 1. Fractional atom coordinates and isotropic-displacement parameters are reported in Table 2 (anisotropic ADPs can be found in the accompanying CIF). Selected bond distances are listed in Table 3. The calculated powder-diffraction pattern, based on the atom coordinates and occupancies reported in

Table 2, is provided in Table 4. A table of structure factors has been deposited with the Principal Editor of *Mineralogical Magazine* and is available at http://www.minersoc.org/pages/e_journals/dep_mat_mm.htm

Chemical composition

Qualitative chemical analysis, using energy-dispersive spectrometry, on the crystal fragment used for the structural study (sample no. I/53a/2312), showed that the only elements present (with $Z > 9$) were Ag, S, Se, Te and minor Cu. Quantitative chemical compositions were determined by wavelength-dispersive spectrometry (WDS) on a JEOL JXA-8600 electron microprobe. Major and minor elements were determined at 20 kV accelerating voltage and 15 nA beam current with a 2 μm beam diameter and 15 s counting times. The following lines were used: $\text{AgL}\alpha$, $\text{CuK}\alpha$, $\text{SK}\alpha$, $\text{SeL}\alpha$ and $\text{TeL}\alpha$. The standards were Ag metal (Ag), Cu metal (Cu), pyrite (S), synthetic PtSe_2 (Se) and synthetic Sb_2Te_3 (Te). The crystal fragment was found to be homogeneous to within analytical errors. The mean composition (8 analyses of different spots) together with wt.% ranges of elements are reported in Table 5. On the basis of 6 atoms, the empirical formula of this specimen of aguilarite is $(\text{Ag}_{3.98}\text{Cu}_{0.02})(\text{Se}_{0.98}\text{S}_{0.84}\text{Te}_{0.18})$.

Chemical analyses of the four other samples reported in Table 5 were carried out at the University of Texas at El Paso using a Cameca

 TABLE 3. Selected bond distances (\AA) for aguilarite (sample # I/53a/2312).

Ag1–X	2.4996(5)	Ag2–X	2.5382(4)	Ag1–Ag2	3.0184(3)
Ag1–X	2.5213(5)	Ag2–X	2.6526(5)	Ag1–Ag2	3.1442(4)
<Ag1–X>	2.5105	Ag2–X	2.6936(5)	Ag1–Ag2	3.1748(5)
		<Ag2–X>	2.6281	Ag1–Ag2	3.1750(3)

TABLE 4. Calculated X-ray powder-diffraction data for agularite (sample # I/53a/2312).

<i>I</i>	<i>d</i> _{calc}	<i>h</i>	<i>k</i>	<i>l</i>
5	3.9956	$\bar{1}$	0	1
5	3.4631	$\bar{1}$	1	1
52	3.0909	1	1	1
58	2.8742	$\bar{1}$	1	2
37	2.6711	1	2	0
95	2.6206	$\bar{1}$	2	1
63	2.6047	0	2	2
31	2.4721	1	1	2
32	2.4568	0	1	3
100	2.4477	1	2	1
86	2.4241	$\bar{1}$	0	3
43	2.2206	0	3	1
7	2.1042	1	2	2
14	2.0947	0	2	3
45	2.0910	2	0	0
22	2.0670	1	0	3
20	2.0021	2	1	0
5	1.9956	0	3	2
8	1.9875	$\bar{1}$	2	3
23	1.9811	1	1	3
11	1.9199	$\bar{2}$	1	2
13	1.8952	0	1	4
6	1.7394	$\bar{2}$	1	3
11	1.7358	0	4	0
27	1.7315	$\bar{2}$	2	2
10	1.7134	0	2	4
5	1.5957	$\bar{2}$	2	3
7	1.5921	$\bar{1}$	4	1
7	1.5885	0	4	2
7	1.5613	$\bar{2}$	3	1
12	1.5369	0	1	5
10	1.4861	2	3	1
8	1.4772	2	1	3
22	1.4761	$\bar{1}$	3	4
8	1.4513	1	4	2
5	1.4113	$\bar{1}$	4	3
15	1.3557	1	3	4
9	1.3538	$\bar{2}$	1	5
6	1.3418	$\bar{2}$	4	1
7	1.3319	$\bar{3}$	0	3
5	1.3117	$\bar{1}$	5	1
8	1.3092	3	1	1
7	1.2994	2	1	4
7	1.2711	$\bar{1}$	5	2
6	1.2239	2	4	2
5	1.1443	$\bar{2}$	2	6
5	1.0972	$\bar{3}$	4	1
5	1.0968	3	3	4

The calculated X-ray powder pattern was computed on the basis of $a = 4.2478(2)$, $b = 6.9432(3)$, $c = 8.0042(5)$ Å, $\beta = 100.103(2)^\circ$, and with the atom coordinates and site occupancies reported in Table 2. Intensities calculated using *XPOW* software version 2.0 (Downs *et al.*, 1993). Only those reflections with $I_{\text{calc}} > 5$ are listed.

SX-50 electron microprobe, operating at 15 kV, 15 nA with a 10 μm beam diameter and 20 s counting times. The analytical standards were pure Ag and Se, and marcasite for S.

Results and discussion

Description of the crystal structure

The crystal structure of agularite (Fig. 1) is topologically identical to that of acanthite (Frueh, 1958). It can be described as a body-centred array of tetrahedrally coordinated *X* atoms (*X* = S, Se and Te) with Ag_2X_3 triangles in planes nearly parallel to (010); the sheets are linked by the Ag1 silver site, which has twofold coordination. The mean bond distances for the two silver sites [i.e. $\langle \text{Ag1}-\text{X} \rangle = 2.511$ Å and $\langle \text{Ag2}-\text{X} \rangle = 2.628$ Å] are slightly longer than those in acanthite [$\langle \text{Ag1}-\text{S} \rangle = 2.503$ Å and $\langle \text{Ag2}-\text{S} \rangle = 2.602$ Å; Frueh (1958)], as a result of the larger radii of Se and Te (Shannon, 1976). The shortest Ag–Ag distance in agularite (Ag1–Ag2 = 3.0184 Å) is nearly identical to the corresponding value in acanthite [Ag1–Ag2 = 3.036 Å, Frueh (1958)]. In naumannite the shortest Ag–Ag distance is 2.93 Å, a value very similar to those in *fcc* silver [$r_{(\text{Ag}-\text{Ag})} = 2.89$ Å; Suh *et al.*, 1988] and *hcp* silver [$r_{(\text{Ag}-\text{Ag})} = 2.93$ Å; Petruk *et al.*, 1970]. The mean electron number refined for the *X* position [0.333(3)S + 0.667Se = 28.01] is in excellent agreement with the value calculated from chemical data (0.49Se + 0.42S + 0.09Te = 28.06).

Comparison of natural and synthetic 'agularite' specimens

A comparison of the *d*-spacings (Table 6) of historic agularite specimens with those of synthetic samples (taken from Pingitore *et al.*, 1992) indicates an acanthite-type structure with a composition close to Ag_4SeS for samples Genth 48a.2 and USNMNH C 380. Electron-probe microanalysis (Table 5) yielded normalized (to an ideal total of 2) anion fractions of $\text{S}_{0.95}\text{Se}_{1.08}$ and $\text{S}_{1.03}\text{Se}_{0.93}$, respectively; these are consistent with the X-ray data. The second studied sample from the NMNH collection (no. 93436) is also from Mexico but there is no further locality information. Its X-ray diffraction pattern is similar to that of naumannite, with some substitution of S for Se. Electron-probe microanalysis (Table 5) indicates anion fractions of $\text{S}_{0.19}\text{Se}_{1.73}$, and therefore this sample is naumannite with ~10%

CRYSTAL STRUCTURE OF AGUILARITE

 TABLE 5. Electron microprobe data [means in wt.% of elements with standard deviations (σ)] together with the crystal-chemical formulae on the basis of 6 atoms for aguilarite crystals.

	I/53a/2312 8	Genth 48a.2 13	Genth 48a.6 12	USNMNH C 380 13	USNMNH 93436 6
Ag	76.5(2)	79.0(3)	78.3(8)	80.1(3)	74.9(1)
Cu	0.23(4)	n.d.	n.d.	n.d.	n.d.
S	4.80(7)	5.6(4)	7.1(1.8)	6.1(2)	1.0(1.0)
Se	13.79(8)	15.8(4)	13.4(1.1)	13.5(2)	23.2(9)
Te	4.10(6)	n.d.	n.d.	n.d.	n.d.
Total	99.42(2)	100.4(3)	98.8(1.0)	99.6(1.0)	99.1(7)
Ag	3.98	3.97	3.90	4.04	4.08
Cu	0.02	—	—	—	—
S	0.84	0.95	1.19	1.03	0.19
Se	0.98	1.08	0.91	0.93	1.73
Te	0.18	—	—	—	—

The second row is the number of analyses; n.d. = not determined.

substitution of S for Se. The Genth 48a.6 specimen produced an X-ray powder pattern similar to those of USNMNH C 380 and Genth 48a.2, with idealized anion fractions of $S_{1.19}Se_{0.91}$.

A comparison of the d -spacings determined for one of the synthetic compounds described by Pingitore *et al.* (1992) of composition Ag_4SeS , with the Genth 48a.2 and USNMNH C 380

specimens, and the aguilarite studied by Petruk *et al.* (1974) is given in Table 6. Note the close correspondence between the values listed for synthetic Ag_4SeS (Pingitore *et al.*, 1992) and those measured for the two museum specimens from San Carlos mine. All three of these are also a credible match to the d -spacings listed for aguilarite by Petruk *et al.* (1974).

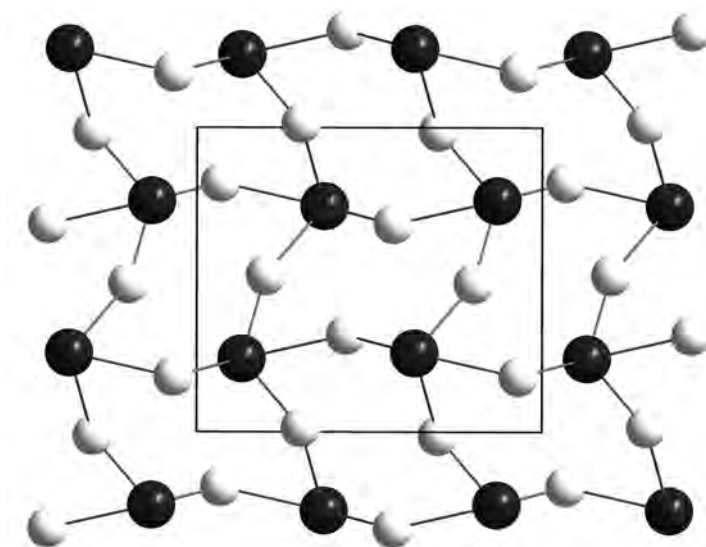


FIG. 1. The crystal structure of aguilarite projected down [100]. The horizontal direction is the c axis. The Ag and X (S, Se and Te) atoms are shown as white and black spheres, respectively. The unit cell is outlined.

TABLE 6. Comparison of X-ray powder diffraction data and indexing of synthetic Ag_4SeS and agularite*.

Acanthite JCPDS 14-72		Ag ₄ SeS synthetic	Agularite NMNH C 380	Agularite Genth 48a.2	Agularite Petruk <i>et al.</i> (1974)	Naumannite JCPDS 241041
3.437	35	3.461	<10	3.467	<10	
3.383	20	3.086	20	3.101	20	111
3.080	60	3.086	20	3.101	20	70
2.836	70	2.878	60	2.895	90	2.737
2.664	45	2.670	30	2.680	40	2.673
2.606	100	2.619	40	2.632	50	2.581
2.583	70	2.583	20	2.618	20	85
2.456	70	2.457	60	2.473	100	
2.440	80	2.446	60	2.451	80	
2.421	60	2.433	100	2.447	80	
2.383	75			2.350	<10	013
		2.294	10	2.304	20	
2.213	45	2.220	30	2.228	40	
						2.254
2.093	16					2.238
2.083	45	2.092	30	2.098	40	17
2.072	16			2.074	10	113
2.047	16					34
1.995	16	1.995	20	2.002	40	2.080
1.963	20	1.984	20	1.986	30	023,301
1.866	16	1.897	10	1.905	20	2.067
						2.014
						2.001
						1.881
1.733	12	1.735	10	1.741	30	23
1.718	20			1.715	10	123
1.587	14	1.598	<10	1.591	<10	014
1.579	10	1.589	<10	1.567	<10	212,132
1.513	12					1.719
						06
1.483	10	1.478	10	1.483	20	1.594
1.470	10	1.473	10	1.442	10	06
1.459	14					1.562
						06
						1.475
						04
5 minors, 1.31-1.38		1.356	<10	1.358	<10	1.475
						04
						2.302
						1.35
						20
						302

* d -spacings are listed in Å, with relative intensities based on 100. The indices, hkl , are based on a monoclinic acanthite-type cell for: synthetic Ag_4SeS , USNMNH C 380 agularite, and Genth 48a.2 agularite; indexing is based on a naumannite-type orthorhombic cell for the Petruk *et al.* (1974) agularite. Petruk *et al.* (1974) agularite also is listed as JCPDS 27-620. Possible minor peaks (<10) on the Genth 48a.2 pattern, not indexed, are at approximately 3.36 (quartz?) and 1.93 Å. ** This d -spacing is likely to be due to contamination by quartz; it is very close to the 3.34 Å spacing of the 1100 peak for that common mineral.

It is apparent that all four of these specimens have essentially identical structures; only one minor ($I = 1$) aguilareite peak listed by Petruk *et al.* (1974) at 3.33 Å is not matched reasonably in the synthetic, Genth and USNMNH specimens. This peak was not reported by Earley (1950) and may be due to a contaminant phase. The quartz I_{100} peak corresponds closely to this spacing (3.34 Å) and Petruk *et al.* (1974) reported that their Guanajuato material was “disseminated in dark grey quartz”.

We have identified a number of peaks that were not documented by Petruk *et al.* (1974). Our diffractometer produces higher resolution data than the powder camera used by Petruk *et al.* (1974). In early analyses using a Gandolfi camera we were unable to resolve some multiple peaks, such as those with d -spacings of 2.457, 2.446 and 2.433 Å. We conclude that the structure of aguilareite reported by Petruk *et al.* (1974) is identical to that of compounds with the same stoichiometry which we produced in the laboratory and with the Genth and USNMNH San Carlos mine aguilareite specimens; they are all the same phase.

Natural and synthetic aguilareite form by an unquenchable solid-state transition from a presumably continuous solid solution (ranging in composition from Ag_2S to Ag_2Se) which is stable at elevated temperatures. The commonly observed cubic morphology of ‘acanthite pseudomorphs after argentite’ document this transition in nature; calorimetry and the similarly cubic morphology of our synthetic phases do the same in the laboratory. For this reason, we do not believe that natural hydrothermal aguilareite differs significantly from synthetic material; both experience the same phase transition. However, the precise boundaries of the two-phase zone between the acanthite- and naumannite-type solid solutions may be affected by the disparity in the rates of cooling in laboratory and natural settings.

Indexing of aguilareite by Petruk et al. (1974) on the naumannite pattern

The seemingly credible indexing of aguilareite on the orthorhombic naumannite cell achieved by Petruk *et al.* (1974) remains disturbing. Most of their indexing (the narrowest spacings have been omitted) is listed in Table 6. Two points are important in this regard.

First, we suspect that Petruk *et al.* (1974) were unable to resolve some closely spaced multiple

lines on their films, as discussed above. The extra lines would not correspond to any naumannite-type reflection. Second, there is a major internal inconsistency in the results of the aguilareite indexing by Petruk *et al.* (1974). The individual d -spacings (Table 6) and the a , b and c dimensions of their naumannite-indexed aguilareite unit cell are larger, in every case, than the corresponding dimension of the naumannite unit cell (4.33 vs. 4.31 Å for a , 7.09 vs. 7.02 Å for b , and 7.76 vs. 7.71 Å for c). The volume of the naumannite-indexed aguilareite unit cell is thus larger (238.2 vs. 237.6 Å³) than that of naumannite; and the naumannite indexed by Petruk *et al.* (1974) yields an even greater difference, as it has a calculated cell volume of 233.3 Å³. Recalling that S^{2-} is 7% smaller in radius than Se^{2-} , that half of the anion sites in aguilareite are occupied by S rather than Se, and that aguilareite and naumannite were assumed by Petruk *et al.* (1974) to have the same structure, it is impossible for the aguilareite unit cell to have a greater volume than that of naumannite. Clearly, in hindsight, the decision to index aguilareite on a naumannite-type cell was inappropriate.

Indexing of synthetic Ag_4SeS by Pingitore et al. (1992) on the acanthite pattern

The indexing of synthetic Ag_4SeS on an acanthite-type monoclinic unit cell is based on our observation of a gradual and systematic shift in the X-ray diffraction peaks of samples with increasing Se content (see Pingitore *et al.*, 1992). These shifts correspond to an expansion of the lattice dimensions as the larger Se^{2-} anion replaces S^{2-} , following Vegard’s law for solid solutions. Table 6 shows our indexing of both Ag_4SeS and the aguilareite of Petruk *et al.* (1974) on an acanthite-type structure. Compare the d -spacings of these two phases with those of acanthite, in the far left position. Note that the d -spacings in both Ag_4SeS and aguilareite are typically larger than those of acanthite, as expected for Se substitution. The fit for both phases, given the anticipated shifts, is quite reasonable.

Status of aguilareite as a mineral species

The foregoing discussion definitively demonstrates that aguilareite is monoclinic, crystallizing in space group $P2_1/n$, and is therefore isostructural with monoclinic acanthite, rather than

orthorhombic $P2_12_12_1$, naumannite, as previously supposed. Aguilarite remains as a valid mineral species, but it should be described as the Se-analogue of acanthite rather than S-rich naumannite. The crystal structure determination revealed no cation ordering at room temperature. Our conclusions support the hypothesis of Pingitore *et al.* (1992, 1993) that there are two distinct solid solution series: a monoclinic 'acanthite-like' $\text{Ag}_2\text{S}-\text{Ag}_2\text{S}_{0.4}\text{Se}_{0.6}$ series; and an orthorhombic 'naumannite-like' $\text{Ag}_2\text{S}_{0.3}\text{Se}_{0.7}-\text{Ag}_2\text{Se}$ series; and is supported by data gathered on synthetic analogues. Moreover, if unit-cell volumes are plotted against selenium content (Fig. 2) for natural aguilarite (this study) and synthetic compounds of both the series (Pingitore *et al.*, 1992), a clear linear trend is observed, which includes neotype specimen 1/53a/2312, despite its enrichment in tellurium.

In the $\text{Ag}_2\text{S}-\text{Ag}_2\text{Se}$ solid solution at room temperature there is a transition from monoclinic to orthorhombic symmetry between 60 and 70 at.% Se (i.e. between $\text{Ag}_2\text{S}_{0.4}\text{Se}_{0.6}$ and $\text{Ag}_2\text{S}_{0.3}\text{Se}_{0.7}$). As structural studies do not indicate site-specific substitutions, the name aguilarite should be applied to the monoclinic phase with more than 50 at.% Se. Aguilarite is therefore monoclinic with an ideal formula Ag_4SeS and a composition field that extends from 50 at.% Se to the monoclinic-orthorhombic transition.

Possible solid-solution with cervelleite, Ag_4TeS

Cervelleite, Ag_4TeS , is a rare mineral first described by Criddle *et al.* (1989) from

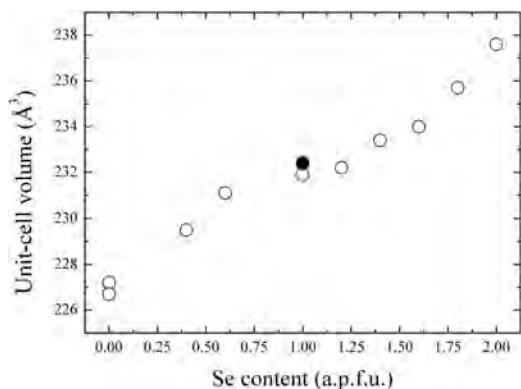


FIG. 2. The unit-cell volume (\AA^3) plotted against the Se content (a.p.f.u.). The filled symbol represents the aguilarite crystal (this study); empty symbols are data from synthetic compounds (Pingitore *et al.*, 1992).

Moctezuma mine, Mexico. Spry and Thieben (1996) subsequently reported a cervelleite-like mineral at the Mayflower epithermal gold-silver telluride deposit in Montana, USA, with an unusual Se-rich composition. The two chemical analyses reported by these authors correspond to a formula $(\text{Ag}_{3.74-3.76}\text{Cu}_{0.08-0.09}\text{As}_{0.00-0.10})_{\Sigma \approx 4}(\text{Te}_{1.11-1.20}\text{S}_{0.66-0.91}\text{Se}_{0.14-0.21})_{\Sigma \approx 2}$, which indicates the possibility of a solid solution, or at least a limited solid solution, between cervelleite and the Se-analogue of cervelleite, aguilarite (Ag_4SeS). Such a feature is strongly corroborated by the chemistry of one of the aguilarite crystals in the present study. Unfortunately, no structural data have been reported either for cervelleite or for synthetic cervelleite-like compounds, the only information being that the mineral may be cubic, with $a = 14.03 \text{ \AA}$ and a primitive lattice (Criddle *et al.*, 1989). As discussed above, members of the $\text{Ag}_2\text{S}-\text{Ag}_2\text{Se}$ system undergo structural transitions to a cubic high-temperature conductive form in the temperature range $70-178^\circ\text{C}$, depending on composition. Full structural data are not available for the high-temperature forms but they are described as cubic with I lattices and unit-cell parameters $a = 4.88(2)$ and $4.98(2) \text{ \AA}$ for Ag_2S and Ag_2Se , respectively (Pingitore *et al.*, 1993). In the light of these data, the unit-cell parameter reported for cervelleite ($a = 14.03 \text{ \AA}$; Criddle *et al.*, 1989), might represent a superstructure with $a_{\text{cervelleite}} = 3a$, the tripling of the cell parameter possibly being due to cation ordering. Such a hypothesis, however, seems unlikely for two reasons: (1) the value of 14.03 \AA is too small with respect to the tripled basic cell parameters observed for the high-temperature cubic forms of Ag_2S and Ag_2Se ; and (2) the high-temperature cubic forms are usually disordered structures (the conductive allotropes) and it would seem unlikely that the superstructure in cervelleite was the result of cation ordering.

Acknowledgements

The paper benefited from reviews by Chris Stanley and Cristian Biagoni. Associate Editor Giancarlo Della Ventura is thanked for his efficient handling of the manuscript. The authors express gratitude to Christopher Holl (Princeton University, USA) who provided the sample used in this study. Thanks are also due to Lincoln Hollister (Princeton University, USA) for bringing the Gem and Mineral Collection hosted in the Department of Geosciences of the Princeton

University to the attention of one of the authors (LB). Deane K. Smith lent two of the 6 original aguilarite specimens from Genth's collection at The Pennsylvania State University for analysis. Pete J. Dunn of the National Museum of Natural History, Washington, D.C., provided two samples of aguilarite. Part of this report is based upon work supported by the US National Science Foundation under grants RII-8922191 and HRD-9450412. The assistance of Benjamin Ponce and Letty Estrada at UTEP is appreciated.

References

- Criddle, A.J. and Stanley, C.J. (editors) (1993) *Quantitative Data File for Ore Minerals*, third edition. Chapman & Hall, London.
- Criddle, A.J., Chisholm, J.E. and Stanley, C.J. (1989) Cerveleite, Ag_4TeS , a new mineral from the Bambolla mine, Mexico, and a description of photo-chemical reaction involving cervelleite, acanthite and hessite. *European Journal of Mineralogy*, **1**, 371–380.
- Davidson, F. (1960) Selenium in some epithermal deposits of antimony, mercury and silver and gold. *U.S. Geological Survey Bulletin*, **1112-A**, 152–164.
- Downs, R.T., Bartelmehs, K.L., Gibbs, G.V. and Boisen, M.B. Jr (1993) Interactive software for calculating and displaying X-ray or neutron powder diffractometer patterns of crystalline materials. *American Mineralogist*, **78**, 1104–1107.
- Earley, J.W. (1950) Description and synthesis of the selenide minerals. *American Mineralogist*, **35**, 337–364.
- Frueh, A.J. Jr (1958) The crystallography of silver sulfide, Ag_2S . *Zeitschrift für Kristallographie*, **110**, 136–144.
- Genth, F.A. (1891) Aguilarite, a new species. *American Journal of Science*, **41**, 401–403.
- Genth, F.A. (1892) Aguilarite. *American Journal of Science*, **44**, 381–383.
- Harcourt, G.A. (1942) Tables for the identification of ore minerals by X-ray powder patterns. *American Mineralogist*, **27**, 63–113.
- Ibers, J.A. and Hamilton, W.C. (editors) (1974) *International Tables for X-ray Crystallography*, vol. IV. Kynock Press, Birmingham, UK, 366 pp.
- Main, J.V., Rodgers, K.A., Kobe, H.W. and Woods, C.P. (1972) Aguilarite from the Camoola Reef, Maratoto Valley, New Zealand. *Mineralogical Magazine*, **38**, 961–964.
- Morales, L.F.V. and Borodayev, Y.S. (1982) New data on minerals of the acanthite–aguilarite–naumannite series. *Doklady Akademi Nauk SSSR*, **264**, 685–688.
- Oxford Diffraction (2006). *CrysAlis RED (Version 1.171.31.2) and ABSPACK in CrysAlis RED*. Oxford Diffraction Ltd, Abingdon, Oxfordshire, UK.
- Petruk, W., Cabri, L.J., Harris, D.C., Stewart, J.M. and Clark, L.A. (1970) Allargentum, redefined. *The Canadian Mineralogist*, **10**, 163–172.
- Petruk, W., Owens, D.R., Stewart, J.M. and Murray, E.J. (1974) Observations on acanthite, aguilarite and naumannite. *The Canadian Mineralogist*, **12**, 365–369.
- Pingitore, N.E., Ponce, B.F., Moreno, F. and Podpora, C. (1992) Solid solutions in the system Ag_2S – Ag_2Se . *Journal of Material Research*, **7**, 2219–2224.
- Pingitore, N.E., Ponce, B.F., Estrada, L., Eastman, M.P., Yuan, H.L., Porter, L.C. and Estrada, G. (1993) Calorimetric analysis of the system Ag_2S – Ag_2Se between 25 and 250°C. *Journal of Material Research*, **8**, 3126–3130.
- Schneiderhöhn, H. and Ramdohr, P. (1931) *Lehrbuch der Erzmikroskopie*, Volume 2. Gebrüder Borntraeger, Berlin, 222 pp.
- Shannon, R.D. (1976) Revised effective ionic radii and systematic studies of interatomic distances in halides and chalcogenides. *Acta Crystallographica*, **A32**, 751–767.
- Sheldrick, G.M. (2008) A short history of *SHELX*. *Acta Crystallographica*, **A64**, 112–122.
- Shikazono, N. (1978) Selenium content of acanthite and the chemical environments of Japanese vein-type deposits. *Economic Geology*, **73**, 524–533.
- Spry, P.G. and Thieben, S.E. (1996) Two new occurrences of benleonardite, a rare silver-tellurium sulphosalt, and a possible new occurrence of cervelleite. *Mineralogical Magazine*, **60**, 871–876.
- Suh, I-K., Ohta, H. and Waseda, Y. (1988) High-temperature thermal expansion of six metallic elements measured by dilatation method and X-ray diffraction. *Journal of Materials Science*, **23**, 757–760.
- Wiegiers, G.A. (1971) The crystal structure of the low-temperature form of silver selenide. *American Mineralogist*, **56**, 1882–1888.
- Xiao, C., Xu, J., Li, K., Feng, J., Yang, J. and Xie, Y. (2012) Superionic phase transition in silver chalcogenide nanocrystals realizing optimized thermoelectric performance. *Journal of the American Chemical Society*, **134**, 4287–4293.

data_new

```
_audit_creation_method          SHELXL-97
_chemical_name_systematic
;
?
;
_chemical_name_common           ?
_chemical_melting_point         ?
_chemical_formula_moiety        ?
_chemical_formula_sum
'Ag2 S0.33 Se0.67'
_chemical_formula_weight        279.11
```

```
loop_
  _atom_type_symbol
  _atom_type_description
  _atom_type_scatter_dispersion_real
  _atom_type_scatter_dispersion_imag
  _atom_type_scatter_source
'Ag' 'Ag' -0.8971 1.1015
'International Tables Vol C Tables 4.2.6.8 and 6.1.1.4'
'S' 'S' 0.1246 0.1234
'International Tables Vol C Tables 4.2.6.8 and 6.1.1.4'
'Se' 'Se' -0.0929 2.2259
'International Tables Vol C Tables 4.2.6.8 and 6.1.1.4'
```

```
_symmetry_cell_setting          ?
_symmetry_space_group_name_H-M  ?
```

```
loop_
  _symmetry_equiv_pos_as_xyz
'x, y, z'
'-x+1/2, y+1/2, -z+1/2'
'-x, -y, -z'
'x-1/2, -y-1/2, z-1/2'
```

```
_cell_length_a                  4.2478(2)
_cell_length_b                   6.9432(3)
_cell_length_c                   8.0042(5)
_cell_angle_alpha                 90.00
_cell_angle_beta                 100.103(2)
_cell_angle_gamma                 90.00
_cell_volume                     232.41(2)
_cell_formula_units_Z             4
_cell_measurement_temperature    293(2)
_cell_measurement_reflns_used    ?
_cell_measurement_theta_min      ?
_cell_measurement_theta_max      ?
```

```
_exptl_crystal_description      ?
_exptl_crystal_colour           ?
_exptl_crystal_size_max         ?
_exptl_crystal_size_mid         ?
_exptl_crystal_size_min         ?
_exptl_crystal_density_meas     ?
_exptl_crystal_density_diffn    7.977
_exptl_crystal_density_method   'not measured'
_exptl_crystal_F_000           488
```

```

_exptl_absorpt_coefficient_mu      27.155
_exptl_absorpt_correction_type     ?
_exptl_absorpt_correction_T_min    ?
_exptl_absorpt_correction_T_max    ?
_exptl_absorpt_process_details     ?

_exptl_special_details
;
?
;

_diffrn_ambient_temperature        293(2)
_diffrn_radiation_wavelength       0.71073
_diffrn_radiation_type              MoK\alpha
_diffrn_radiation_source            'fine-focus sealed tube'
_diffrn_radiation_monochromator     graphite
_diffrn_measurement_device_type     ?
_diffrn_measurement_method         ?
_diffrn_detector_area_resol_mean   ?
_diffrn_standards_number           ?
_diffrn_standards_interval_count   ?
_diffrn_standards_interval_time    ?
_diffrn_standards_decay_%          ?
_diffrn_reflns_number              3832
_diffrn_reflns_av_R_equivalents    0.0661
_diffrn_reflns_av_sigmaI/netI     0.2480
_diffrn_reflns_limit_h_min         -6
_diffrn_reflns_limit_h_max         6
_diffrn_reflns_limit_k_min         -11
_diffrn_reflns_limit_k_max         11
_diffrn_reflns_limit_l_min         -12
_diffrn_reflns_limit_l_max         12
_diffrn_reflns_theta_min           3.91
_diffrn_reflns_theta_max           34.97
_reflns_number_total               958
_reflns_number_gt                   520
_reflns_threshold_expression        >2sigma(I)

_computing_data_collection         ?
_computing_cell_refinement         ?
_computing_data_reduction          ?
_computing_structure_solution      ?
_computing_structure_refinement    'SHELXL-97 (Sheldrick, 1997)'
_computing_molecular_graphics      ?
_computing_publication_material    ?

_refine_special_details
;
Refinement of F2 against ALL reflections. The weighted R-factor wR and
goodness of fit S are based on F2, conventional R-factors R are based
on F, with F set to zero for negative F2. The threshold expression of
F2 > 2sigma(F2) is used only for calculating R-factors(gt) etc. and is
not relevant to the choice of reflections for refinement. R-factors based
on F2 are statistically about twice as large as those based on F, and R-
factors based on ALL data will be even larger.
;

_refine_ls_structure_factor_coef   Fsqd
_refine_ls_matrix_type             full
_refine_ls_weighting_scheme        calc
_refine_ls_weighting_details

```

```
'calc w=1/[\s^2^(Fo^2^)+(0.0556P)^2^+0.1239P] where P=(Fo^2^+2Fc^2^)/3'
_atom_sites_solution_primary      direct
_atom_sites_solution_secondary    difmap
_atom_sites_solution_hydrogens    geom
_refine_ls_hydrogen_treatment     mixed
_refine_ls_extinction_method      none
_refine_ls_extinction_coef        ?
_refine_ls_number_reflns         958
_refine_ls_number_parameters      29
_refine_ls_number_restraints      0
_refine_ls_R_factor_all           0.0152
_refine_ls_R_factor_gt            0.0139
_refine_ls_wR_factor_ref          0.0306
_refine_ls_wR_factor_gt          0.0305
_refine_ls_goodness_of_fit_ref    0.223
_refine_ls_restrained_S_all       0.223
_refine_ls_shift/su_max           0.000
_refine_ls_shift/su_mean          0.000
```

```
loop_
  _atom_site_label
  _atom_site_type_symbol
  _atom_site_fract_x
  _atom_site_fract_y
  _atom_site_fract_z
  _atom_site_U_iso_or_equiv
  _atom_site_adp_type
  _atom_site_occupancy
  _atom_site_symmetry_multiplicity
  _atom_site_calc_flag
  _atom_site_refinement_flags
  _atom_site_disorder_assembly
  _atom_site_disorder_group
Ag1 Ag 0.75442(6) 0.01378(4) 0.30116(2) 0.01762(6) Uani 1 1 d . . .
Ag2 Ag 0.28840(6) 0.31874(4) 0.43144(2) 0.01803(6) Uani 1 1 d . . .
S1 S 0.36028(10) 0.24110(7) 0.13054(4) 0.02162(13) Uani 0.333(3) 1 d P . .
Se1 Se 0.36028(10) 0.24110(7) 0.13054(4) 0.02162(13) Uani 0.667(3) 1 d P . .
```

```
loop_
  _atom_site_aniso_label
  _atom_site_aniso_U_11
  _atom_site_aniso_U_22
  _atom_site_aniso_U_33
  _atom_site_aniso_U_23
  _atom_site_aniso_U_13
  _atom_site_aniso_U_12
Ag1 0.01810(10) 0.01774(12) 0.01705(9) 0.00000(8) 0.00318(7) -0.00012(10)
Ag2 0.01845(11) 0.01826(13) 0.01740(8) 0.00019(8) 0.00317(7) 0.00002(9)
S1 0.0215(2) 0.0222(3) 0.02112(18) -0.00001(15) 0.00385(14) -0.00033(17)
Se1 0.0215(2) 0.0222(3) 0.02112(18) -0.00001(15) 0.00385(14) -0.00033(17)
```

```
_geom_special_details
```

```
;
```

All esds (except the esd in the dihedral angle between two l.s. planes) are estimated using the full covariance matrix. The cell esds are taken into account individually in the estimation of esds in distances, angles and torsion angles; correlations between esds in cell parameters are only used when they are defined by crystal symmetry. An approximate (isotropic) treatment of cell esds is used for estimating esds involving l.s. planes.

```
;
```

loop_
_geom_bond_atom_site_label_1
_geom_bond_atom_site_label_2
_geom_bond_distance
_geom_bond_site_symmetry_2
_geom_bond_publ_flag
Ag1 Se1 2.4996(5) 2_645 ?
Ag1 S1 2.4996(5) 2_645 ?
Ag1 S1 2.5213(5) . ?
Ag1 Ag2 3.0184(3) 2_545 ?
Ag1 Se1 3.1038(5) 4_666 ?
Ag1 Ag2 3.1442(4) 1_655 ?
Ag1 Ag2 3.1750(3) 3_656 ?
Ag1 Ag2 3.1959(3) . ?
Ag1 Ag2 3.2063(3) 4_665 ?
Ag1 Ag2 3.2156(3) 2_645 ?
Ag2 S1 2.5382(4) . ?
Ag2 Se1 2.6526(5) 4_566 ?
Ag2 S1 2.6526(5) 4_566 ?
Ag2 Se1 2.6936(5) 4_666 ?
Ag2 S1 2.6936(5) 4_666 ?
Ag2 Ag1 3.0184(3) 2 ?
Ag2 Se1 3.0224(6) 2 ?
Ag2 Ag1 3.1442(4) 1_455 ?
Ag2 Ag2 3.1748(5) 3_666 ?
Ag2 Ag1 3.1750(3) 3_656 ?
S1 Ag1 2.4996(5) 2_655 ?
S1 Ag2 2.6526(5) 4_665 ?
S1 Ag2 2.6936(5) 4_565 ?

loop_
_geom_angle_atom_site_label_1
_geom_angle_atom_site_label_2
_geom_angle_atom_site_label_3
_geom_angle
_geom_angle_site_symmetry_1
_geom_angle_site_symmetry_3
_geom_angle_publ_flag
Se1 Ag1 S1 0.000(15) 2_645 2_645 ?
Se1 Ag1 S1 160.000(13) 2_645 . ?
S1 Ag1 S1 160.000(13) 2_645 . ?
Se1 Ag1 Ag2 101.250(13) 2_645 2_545 ?
S1 Ag1 Ag2 101.250(13) 2_645 2_545 ?
S1 Ag1 Ag2 65.413(12) . 2_545 ?
Se1 Ag1 Se1 103.757(14) 2_645 4_666 ?
S1 Ag1 Se1 103.757(14) 2_645 4_666 ?
S1 Ag1 Se1 95.759(10) . 4_666 ?
Ag2 Ag1 Se1 138.689(12) 2_545 4_666 ?
Se1 Ag1 Ag2 91.774(14) 2_645 1_655 ?
S1 Ag1 Ag2 91.774(14) 2_645 1_655 ?
S1 Ag1 Ag2 97.466(14) . 1_655 ?
Ag2 Ag1 Ag2 159.277(10) 2_545 1_655 ?
Se1 Ag1 Ag2 50.240(10) 4_666 1_655 ?
Se1 Ag1 Ag2 54.165(11) 2_645 3_656 ?
S1 Ag1 Ag2 54.165(11) 2_645 3_656 ?
S1 Ag1 Ag2 135.171(14) . 3_656 ?
Ag2 Ag1 Ag2 87.803(8) 2_545 3_656 ?
Se1 Ag1 Ag2 80.969(11) 4_666 3_656 ?
Ag2 Ag1 Ag2 112.919(9) 1_655 3_656 ?
Se1 Ag1 Ag2 148.184(12) 2_645 . ?
S1 Ag1 Ag2 148.184(12) 2_645 . ?

S1 Ag1 Ag2 51.063(10) . . ?
Ag2 Ag1 Ag2 92.788(8) 2_545 . ?
Sel Ag1 Ag2 50.602(9) 4_666 . ?
Ag2 Ag1 Ag2 84.129(9) 1_655 . ?
Ag2 Ag1 Ag2 98.616(9) 3_656 . ?
Sel Ag1 Ag2 110.046(12) 2_645 4_665 ?
S1 Ag1 Ag2 110.046(12) 2_645 4_665 ?
S1 Ag1 Ag2 53.571(10) . 4_665 ?
Ag2 Ag1 Ag2 75.321(9) 2_545 4_665 ?
Sel Ag1 Ag2 124.185(13) 4_666 4_665 ?
Ag2 Ag1 Ag2 85.137(8) 1_655 4_665 ?
Ag2 Ag1 Ag2 154.563(11) 3_656 4_665 ?
Ag2 Ag1 Ag2 101.048(8) . 4_665 ?
Sel Ag1 Ag2 50.867(10) 2_645 2_645 ?
S1 Ag1 Ag2 50.867(10) 2_645 2_645 ?
S1 Ag1 Ag2 111.168(11) . 2_645 ?
Ag2 Ag1 Ag2 85.842(8) 2_545 2_645 ?
Sel Ag1 Ag2 135.276(12) 4_666 2_645 ?
Ag2 Ag1 Ag2 90.104(8) 1_655 2_645 ?
Ag2 Ag1 Ag2 101.296(8) 3_656 2_645 ?
Ag2 Ag1 Ag2 159.968(10) . 2_645 ?
Ag2 Ag1 Ag2 59.256(9) 4_665 2_645 ?
S1 Ag2 Sel 138.251(17) . 4_566 ?
S1 Ag2 S1 138.251(17) . 4_566 ?
Sel Ag2 S1 0.00(2) 4_566 4_566 ?
S1 Ag2 Sel 106.410(17) . 4_666 ?
Sel Ag2 Sel 105.224(13) 4_566 4_666 ?
S1 Ag2 Sel 105.224(13) 4_566 4_666 ?
S1 Ag2 S1 106.410(17) . 4_666 ?
Sel Ag2 S1 105.224(13) 4_566 4_666 ?
S1 Ag2 S1 105.224(13) 4_566 4_666 ?
Sel Ag2 S1 0.00(2) 4_666 4_666 ?
S1 Ag2 Ag1 73.502(12) . 2 ?
Sel Ag2 Ag1 84.883(12) 4_566 2 ?
S1 Ag2 Ag1 84.883(12) 4_566 2 ?
Sel Ag2 Ag1 161.124(15) 4_666 2 ?
S1 Ag2 Ag1 161.124(15) 4_666 2 ?
S1 Ag2 Sel 96.128(13) . 2 ?
Sel Ag2 Sel 96.031(14) 4_566 2 ?
S1 Ag2 Sel 96.031(14) 4_566 2 ?
Sel Ag2 Sel 112.805(13) 4_666 2 ?
S1 Ag2 Sel 112.805(13) 4_666 2 ?
Ag1 Ag2 Sel 49.338(10) 2 2 ?
S1 Ag2 Ag1 75.057(12) . 1_455 ?
Sel Ag2 Ag1 64.090(12) 4_566 1_455 ?
S1 Ag2 Ag1 64.090(12) 4_566 1_455 ?
Sel Ag2 Ag1 127.997(14) 4_666 1_455 ?
S1 Ag2 Ag1 127.997(14) 4_666 1_455 ?
Ag1 Ag2 Ag1 70.669(6) 2 1_455 ?
Sel Ag2 Ag1 118.760(12) 2 1_455 ?
S1 Ag2 Ag2 109.957(15) . 3_666 ?
Sel Ag2 Ag2 108.833(14) 4_566 3_666 ?
S1 Ag2 Ag2 108.833(14) 4_566 3_666 ?
Sel Ag2 Ag2 61.352(13) 4_666 3_666 ?
S1 Ag2 Ag2 61.352(13) 4_666 3_666 ?
Ag1 Ag2 Ag2 100.515(12) 2 3_666 ?
Sel Ag2 Ag2 51.453(11) 2 3_666 ?
Ag1 Ag2 Ag2 168.624(14) 1_455 3_666 ?
S1 Ag2 Ag1 121.054(15) . 3_656 ?
Sel Ag2 Ag1 49.814(12) 4_566 3_656 ?
S1 Ag2 Ag1 49.814(12) 4_566 3_656 ?

Se1 Ag2 Ag1 68.984(11) 4_666 3_656 ?
S1 Ag2 Ag1 68.984(11) 4_666 3_656 ?
Ag1 Ag2 Ag1 127.890(12) 2 3_656 ?
Se1 Ag2 Ag1 141.369(11) 2 3_656 ?
Ag1 Ag2 Ag1 67.081(9) 1_455 3_656 ?
Ag2 Ag2 Ag1 116.066(11) 3_666 3_656 ?
S1 Ag2 Ag1 50.593(12) . . ?
Se1 Ag2 Ag1 128.420(14) 4_566 . ?
S1 Ag2 Ag1 128.420(14) 4_566 . ?
Se1 Ag2 Ag1 62.927(11) 4_666 . ?
S1 Ag2 Ag1 62.927(11) 4_666 . ?
Ag1 Ag2 Ag1 123.083(8) 2 . ?
Se1 Ag2 Ag1 135.466(11) 2 . ?
Ag1 Ag2 Ag1 84.129(9) 1_455 . ?
Ag2 Ag2 Ag1 107.006(12) 3_666 . ?
Ag1 Ag2 Ag1 81.384(9) 3_656 . ?
Ag1 S1 Ag1 90.492(14) 2_655 . ?
Ag1 S1 Ag2 79.326(13) 2_655 . ?
Ag1 S1 Ag2 78.344(12) . . ?
Ag1 S1 Ag2 76.021(14) 2_655 4_665 ?
Ag1 S1 Ag2 76.543(14) . 4_665 ?
Ag2 S1 Ag2 144.352(19) . 4_665 ?
Ag1 S1 Ag2 137.24(2) 2_655 4_565 ?
Ag1 S1 Ag2 131.92(2) . 4_565 ?
Ag2 S1 Ag2 110.367(18) . 4_565 ?
Ag2 S1 Ag2 105.223(13) 4_665 4_565 ?

_diffirn_measured_fraction_theta_max 0.936
_diffirn_reflns_theta_full 34.97
_diffirn_measured_fraction_theta_full 0.936
_refine_diff_density_max 1.263
_refine_diff_density_min -1.406
_refine_diff_density_rms 0.192